Selective Collective Emission from a Dense Atomic Ensemble Coupled to a Nanophotonic Resonator

Xinchao Zhou,[1] Deepak A. Suresh,[1] F. Robicheaux,[1,2] and Chen-Lung Hung[1,2,*]
[1]Department of Physics and Astronomy, Purdue University, West Lafayette, Indiana 47907, USA
[2]Purdue Quantum Science and Engineering Institute, Purdue University, West Lafayette, Indiana 47907, USA

(Received 31 March 2025; revised 11 July 2025; accepted 14 August 2025; published 10 September 2025)

We experimentally and theoretically study collective emission of a dense atomic ensemble coupled to a single mode in a nanophotonic microring resonator. Because many cold atoms are localized in a small volume, these trapped atoms collectively couple not only to the guided resonator mode but also to the nonguided modes in free space. Through tuning the atom-photon coupling and by adjusting the number of trapped atoms, we demonstrate superradiant emission to the microring resonator. For photon emission via the nonguided modes, our study reveals signatures of subradiance and superradiance when the system is driven to the steady state and to the timed-Dicke state, respectively. Our experimental platform thus presents the first atom-light interface with selective collective emission behavior into a guided mode and the environment. Our observation and methodology could shed light on future explorations of collective emission with densely packed quantum emitters coupled to nanophotonic light-matter interfaces.

DOI: 10.1103/cdd5-r7h4

Collective interaction between single photons and an atomic ensemble has been widely explored in quantum optics [1–3]. Experimental advances hold the promise for enhancing atom-light interfaces, which are crucial for applications in quantum memory, entanglement generation, quantum teleportation [4], as well as for quantum sensing and metrology [5,6]. It is essential to engineer collective photon emission within the interface and minimize coupling to the environment. This approach helps to protect quantum coherence in various applications [7–9].

Superradiant and subradiant emissions are quintessential collective phenomena, characterized by spontaneous emission rates that are either enhanced or suppressed relative to single atom decay. Numerous experiments have validated these effects by exciting atoms and analyzing the photon emission dynamics along well-defined modes. These modes are typically defined by free space collection optics, as seen in most atomic ensemble studies [10–18], or by coupling to an optical cavity or a nanophotonic waveguide [19–24]. While most experiments focus on demonstrating collective effects via a selected photonic mode, a comprehensive study including the collective emission to all other noncollected modes, that is, the environment, has remained elusive.

Interestingly, densely packed atoms could exhibit novel collective emission into the environment due to the interplay between phase-matching conditions and long-range dipole-dipole interactions. Hence, the atoms can selectively couple to a specific photonic mode of interest while exhibiting different collective emission behavior to the environment. One significant example is the "selective radiance" in a subwavelength-spaced atom array. For instance, an atom array trapped along a nanophotonic waveguide can be driven by a weak pulse through a waveguide mode with wave number k_{wg} larger than the free space wave number k_0. The photon emission rate into the same mode $R_c \propto N$ can be superradiantly enhanced, where N is the number of atoms, while the emission rate into all nonguided (free space) modes R_f becomes polynomially or even exponentially suppressed with respect to increasing N due to phase mismatch and destructive interference [25]. For randomly distributed atoms, on the other hand, dipole-dipole interactions could dephase coherence in the excited state, leading instead to faster than single-atom decay rate into free space modes [26].

In this Letter, we present the first experimental study of an atom-light interface showing selective collective emission behavior into a waveguide mode and the environment, respectively. We study a novel system featuring a dense atomic ensemble collectively coupled via dipole-dipole interactions, mediated by a traveling-wave cavity mode (whispering-gallery mode) of a nanophotonic microring resonator and the nonguided modes in free space. We monitor the collective emission dynamics following long and short excitation pulses, with the former driving the atomic ensemble into the steady state (SS) and the latter approximately into the so-called timed-Dicke state (TDS) [7,27,28]. The TDS is described by a phase-correlated spin wavelike excitation $(1/\sqrt{N})\sum_j c_j e^{i\vec{k}\cdot\vec{r}_j}|g_1 \cdots e_j \cdots g_N\rangle$ of wave vector $\vec{k}$ [29], where g_j (e_j) denotes the ground

*Contact author: clhung@purdue.edu

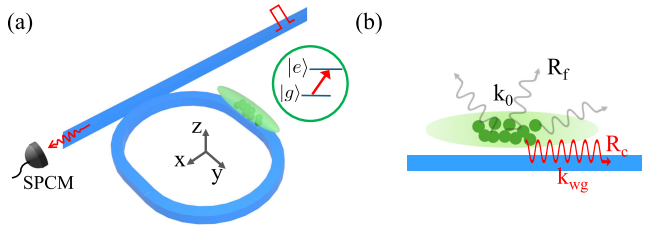

FIG. 1. Schematic of the experimental setup. (a) A dense atomic cloud is trapped above a nanophotonic microring resonator, interacting with a single resonator mode via a cycling transition denoted by $|g\rangle \leftrightarrow |e\rangle$. Resonant pulses are sent through a bus waveguide to excite the resonator mode and the atoms. Transmitted photon counts are detected by a single photon counting module (SPCM). (b) Cross-sectional view (in the y-z plane). R_c denotes photon emission rate to the resonator mode of wave number $k_{\mathrm{wg}} > k_0$, where k_0 is the wave number in free space. R_f is the emission rate into all nonguided modes.

(excited) state of the jth atom and the coefficient c_j is proportional to the driving amplitude at each atomic position $\vec{r}_j$; $c_j = 1$ for a TDS excited by a plane wave and atoms can superradiantly emit a photon along the direction $\vec{k}$ following excitation [7]. Using these two conditions, we discuss how signals collected solely from the resonator could reveal the collective emission dynamics in the noncollected modes as well. Specifically, we demonstrate superradiant decay to the resonator and reveal signatures of subradiance (for the steady state) and superradiance (for the timed-Dicke state) for atomic decay to the nonguided modes.

Our experiment starts from $N \lesssim 60$ cesium atoms laser cooled into a microtrap on a microring resonator with a low temperature ~23 μK and spin polarized in the ground state $|g\rangle \equiv |F = 4, m_{\mathrm{F}} = 4\rangle$ [24]. The root-mean-square size of the atomic cloud is $(0.1\lambda_0, 2.3\lambda_0, 0.5\lambda_0)$ along three trap axes shown in Fig. 1(a), where $\lambda_0 \approx 852.3$ nm is the transition wavelength. The microring is formed using a Si_3N_4 waveguide on a SiO_2 substrate [33], supporting a traveling-wave mode with a wave number $k_{\mathrm{wg}} = n_{\mathrm{eff}} k_0$ and $n_{\mathrm{eff}} \approx 1.7$ is the effective refractive index. The guided mode is circularly polarized and couples to the trapped atoms via the $|g\rangle \leftrightarrow |e\rangle \equiv |F' = 5, m_{F'} = 5\rangle$ cycling transition [24]. We operate in the bad cavity limit, where the resonator decay rate $\kappa \approx 2\pi \times 1.7$ GHz is much larger than the variable atom-photon coupling rate $g \lesssim 2\pi \times 8$ MHz and the single atom decay rate $\Gamma_0 \approx 2\pi \times 5.2$ MHz. To reveal the emission dynamics through the free space modes, the coupling rate g is purposely tuned smaller than Γ_0 by increasing the trap position $z_0 \gtrsim 400$ nm above the waveguide surface. Within the photon emission time scale, each atom would displace by $\lesssim 2$ nm within the trap, effectively frozen in space.

In each experiment, we send a resonant laser pulse into a bus waveguide to excite the microring and drive the atoms. Following weak (much less than one) excitation, the excited population decays by collectively emitting a photon either into the guided resonator mode or to other nonguided modes, as depicted in Fig. 1(b). We detect emitted photons via the bus waveguide using a single photon counting module; those in the nonguided modes are not detected. For single atoms, the figure-of-merit ratio R_c/R_f (signal versus loss to the environment) is given by the single-atom cooperativity $C_1 = 4g^2/\kappa\Gamma_0$. For many atoms, this ratio becomes NC_1 when considering N atoms superradiantly couple to the microring while independently emitting into free space. We explore collective emission within the range $0 \lesssim NC_1 \lesssim 2$. We notice that a small backscattering effect is present in our microring, weakly coupling the traveling-wave mode to a counterpropagating mode that interacts poorly with the spin-polarized atoms. Throughout the Letter, the quoted values of C_1 include a reduction factor of ≈0.7 due to back scattering and are weight-averaged based on the calculated spatial variation of g over the trap density distribution [24].

We note that collective emission from elongated atomic ensembles into free space has recently been studied [17,18,34]. Our study introduces a nanophotonic interface with a resonant wave number significantly larger than k_0, allowing us to directly create excitations phase mismatched with free space modes. For typical experiments in free space, TDS-like spin wave excitations with large wave numbers $k > k_0$ are difficult to prepare directly. This was recently achieved using a sequence of fast pulses [18] and the subsequent decay dynamics was studied in Refs. [18,26].

Theoretical model—We first investigate the theoretical properties of the collective states weakly excited using the microring resonator. Specifically, we calculate the dynamics of N atomic dipoles interacting via a single-mode traveling wave cavity and the nonguided radiation modes by also considering the spatial variation of atom-photon coupling rate [29,35]. In this model, the amplitudes of the atomic dipole moments, when written in a vector form $\vec{\sigma} = \{\sigma^1, \ldots, \sigma^N\}$, follow a system of coupled equations which has been solved in an eigenvalue problem [25,36–39]. Hence, time evolution of the dipoles can be expressed as $\vec{\sigma}(t) = \sum_{\xi=1}^{N} w_\xi e^{i\lambda_\xi t} \vec{v}_\xi$, where $\vec{v}_\xi$ is the eigenvector labeled by $\xi \in [1, \ldots, N]$, w_ξ is the amplitude of the populated eigenvector, and λ_ξ is the eigenvalue. The real part of λ_ξ represents the energy of the state, that is, the collective Lamb shift and the imaginary part relates to the collective decay rate $\Gamma_\xi = 2\,\mathrm{Im}[\lambda_\xi]$ when the system is initially excited *purely* to an eigenvector $\vec{v}_\xi$.

Figures 2(a) and 2(b) show sample distributions of the populated eigenvectors in the steady state and the timed-Dicke state, respectively, labeled using the decay rate Γ_ξ. We see that the steady state is primarily populated with the subradiant eigenstates with decay rate slower than

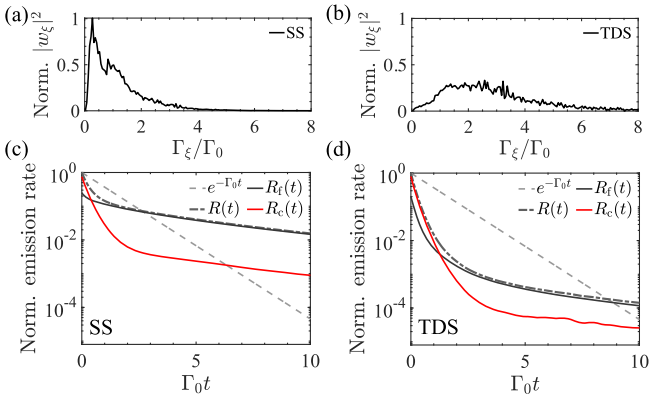

FIG. 2. Calculated collective emission properties of the system. (a),(b) Normalized eigenstate population $|w_\xi|^2$ for (a) the steady states (SS) and (b) the timed-Dicke states (TDS) as a function of decay rate Γ_ξ, respectively. The distribution is sampled using 5000 random configurations of $N = 50$ atoms in the trap [24] with an averaged single-atom cooperativity $C_1 = 0.05$. (c),(d) Time evolution of ensemble-averaged photon emission rates, $R_c(t)$ (red curves) and $R_f(t)$ (black curves), of (c) the SS and (d) the TDS, respectively. Dash-dotted curves mark the total emission rates $R(t)$. Dashed lines mark single atom decay in free space.

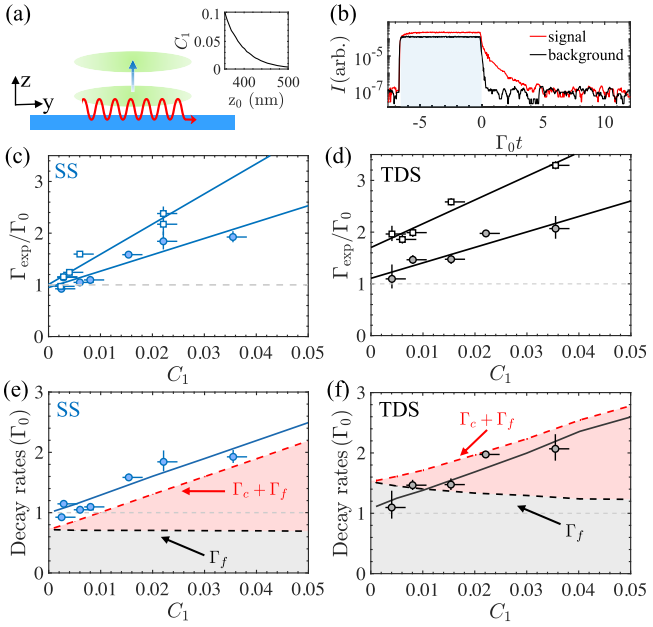

FIG. 3. C_1 dependence of the decay rate measured from the guided mode. (a) Tuning atom-photon coupling strength by changing the trap location. The inset shows the averaged single-atom cooperativity C_1 versus the trap center z_0. (b) Sample photon count traces with (red) and without (black) the presence of trapped atoms. (c),(d) Fitted decay rate Γ_{exp} versus C_1 at a fixed atom number (symbols) of (c) the steady state (SS) with $N = 32 \pm 5$ (filled circles), 58 ± 8 (open squares), and (d) the timed-Dicke state (TDS) with $N = 30 \pm 7$ (filled circles), 46 ± 5 (open squares), respectively. Solid lines are linear fits. (e),(f) Calculated decay rate Γ_{th} (solid lines) of $N = 30$ atoms. Measured Γ_{exp} [symbols as in (c), (d)] are plotted for comparison. As indicated, red (black) dashed lines show the decay rate of photon emission Γ (Γ_f).

single-atom decay, $\Gamma_\xi \lesssim \Gamma_0$, while the timed-Dicke state is mainly populated by the superradiant states ($\Gamma_\xi \gtrsim \Gamma_0$).

Given the state vector $\vec{\sigma}(t)$, we can then evaluate the photon emission rates to the resonator and the free space modes, $R_c(t)$ and $R_f(t)$, respectively, as illustrated in Figs. 2(c) and 2(d). We note the total photon emission rate $R(t) = R_c(t) + R_f(t)$ is essentially the population deexcitation rate due to the conservation of energy [29]. For single atom emission, R, R_c, and R_f should all decay single exponentially at the Purcell-enhanced decay rate $(C_1 + 1)\Gamma_0$. Here, we focus on analyzing the *time evolution* of the ensemble-averaged photon emission rates, as a typical photon count trace $I(t) \propto R_{c,f}(t)$ can faithfully record the time dependence of the emission rate. Direct measurement of the absolute rate requires accurate calibrations of the photon collection efficiencies. For a reference, we compare time dependence of R_c and R_f with a single atom decay curve in free space. In both the steady state (c) and the timed-Dicke state (d), $R_c(t)$ decreases with an exponential rate faster than Γ_0 in the early time $\Gamma_0 t \lesssim 2$, suggesting superradiant emission. For emission into free space, the SS and the TDS show different dynamics: for the SS, $R_f(t)$ decreases at a rate that is initially comparable to, and later slower than, single-atom decay. The later time behavior is typically identified as a signature of subradiance [10–14,20]. For the TDS, $R_f(t)$ initially decreases faster than single-atom decay before transitioning to a subradiant behavior. The fast initial decrease of $R_f(t)$ is due to dephasing in the spin wave of the timed-Dicke state, as observed and discussed in Refs. [18,26].

Experiment and theory comparison—C_1 dependence— We experimentally characterize the rates of collective emission into the microring resonator and free space, respectively. As discussed, we collect photons solely from the resonator. To reveal the emission dynamics in the nonguided modes, we measure the decay rates while reducing the strength of the interaction through the guided mode and approximately maintaining the free space dipole-dipole interaction. To do this, we fix the atom number and increase the distance between the trapped atoms and the waveguide surface, as illustrated in Fig. 3(a), by increasing the strength of an evanescent-wave repulsive potential to move the trap center z_0 away from the waveguide [24]. We study atoms trapped at $z_0 \gtrsim 400$ nm and have verified numerically that the dipole-dipole interaction from the nonguided mode contributions can be well approximated by the free space Green's function, with diminishing perturbation from the surface scattering contributions [29]. The inset of Fig. 3(a), on the other hand, shows the exponential reduction of the atom-resonator interaction with increasing z_0.

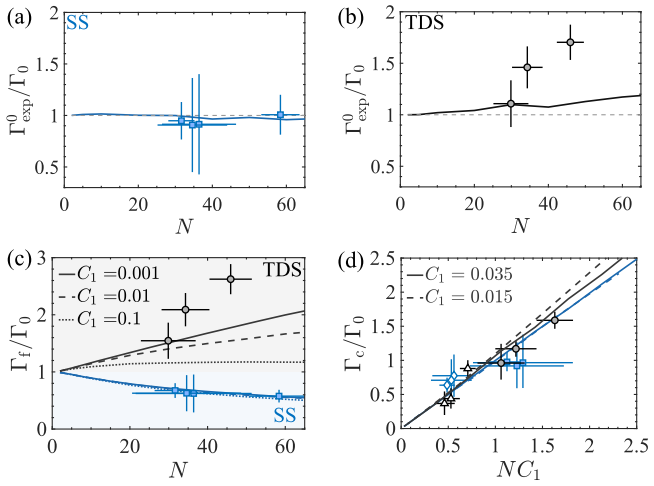

FIG. 4. Selective collective emission. (a),(b) Experimentally extracted $\Gamma^0_{\rm exp}$ (symbols) versus atom number N for (a) the steady state (SS) and (b) the timed-Dicke state (TDS), respectively. Solid lines show $\Gamma_{\rm th}$ in the limit of $C_1 \to 0$. (c) $\Gamma_f = \Gamma^0_{\rm exp}/\theta$ of the SS (filled circles) and the TDS (filled squares), evaluated using the experimental data $\Gamma^0_{\rm exp}$ as shown in (a),(b) and θ evaluated from the theoretical model. Blue (black) lines are numerical calculations using Eq. (1) for the SS (TDS) with the indicated single-atom cooperativity C_1. (d) $\Gamma_c \approx \Gamma_{\rm exp} - \Gamma^0_{\rm exp}$ for the SS (blue symbols) and the TDS (gray symbols), measured at $C_1 = 0.035$ (filled symbols) and 0.015 (open symbols), respectively. Blue (black) lines are numerical calculations for the SS (TDS) using Eq. (1) with the corresponding C_1, showing $\Gamma_c/\Gamma_0 \approx NC_1$.

Figure 3(b) shows samples of the measured photon count trace $I(t)$. We drive the system into the steady state using a pulse width of 200 ns $\sim 6/\Gamma_0$. For approximately exciting the timed-Dicke state, we employ pulses with a full width at half maximum of 6 ns; see [29]. We focus on the early-time dynamics after the pulse is switched off at $t = 0$ and assume $I(t) \propto R_c(t) \sim e^{-\Gamma_{\rm exp} t}$. For $t \gtrsim 2/\Gamma_0$, the signal approaches a small background mainly contributed by residual nonfiltered trap light [40]. We perform exponential fits with a constant offset and extract the signal decay rate $\Gamma_{\rm exp}$.

Figures 3(c) and 3(d) show the C_1 dependence of the fitted $\Gamma_{\rm exp}$ for the steady state and the timed-Dicke state, respectively. We measure the emission dynamics to the lowest possible value of C_1 allowed by the signal-to-noise ratio. Here, uncertainties in the values of C_1 primarily stem from the uncertainty in the dipole trap power which shifts the trap center. Fixing the atom number, the measured decay rate decreases approximately linearly with smaller C_1 and the fitted slope can be used to determine the trapped atom number N, a relation that we further confirm in Fig. 4(d). In Figs. 3(e) and 3(f), we have plotted the early-time decay rates $\Gamma_{\rm th}$ (solid lines) of R_c calculated from the theoretical model. These values agree with the measurement results at the given atom number N.

From linear extrapolations of the measured decay rates to $C_1 = 0$, we can deduce the limit $\Gamma^0_{\rm exp} \equiv \Gamma_{\rm exp}(C_1 \to 0)$ when the free space dipole-dipole interactions become dominant. For the steady state, we measure $\Gamma^0_{\rm exp} \approx \Gamma_0$. For the timed-Dicke state, $\Gamma^0_{\rm exp} \gtrsim \Gamma_0$ is observed. The two states display different magnitudes of the decay rate $\Gamma^0_{\rm exp}$ and different number dependence; see Fig. 4.

A naive interpretation of $\Gamma^0_{\rm exp}$ is that this reveals the excitation decay rate due to photon emission into free space. To see if the answer is as straightforward as it seems, we note that the (early-time) total decay rate of a collective excitation can be operationally defined as $\Gamma = -d[\ln R(t)]/dt = -\dot{R}(t)/R(t)$, following the fact that our experiments measure the decay of the photon emission rates. We then define

$$\Gamma_c = -\frac{\dot{R}_c(t)}{R(t)} \quad \text{and} \quad \Gamma_f = -\frac{\dot{R}_f(t)}{R(t)}, \tag{1}$$

where $\Gamma = \Gamma_c + \Gamma_f$ and Γ_c (Γ_f) is the contribution through emitting to the resonator mode (the nonguided modes). The measured decay rate $\Gamma_{\rm exp}$ and the calculated decay rate $\Gamma_{\rm th}$ from the theoretical model are thus related to these rates as

$$\Gamma_{\rm exp} \approx \Gamma_{\rm th} = -\frac{\dot{R}_c(t)}{R_c(t)} = \Gamma_c + \Gamma_f \theta, \tag{2}$$

where $t = 0$ and $\theta = (\dot{R}_c/R_c)/(\dot{R}_f/R_f)$ takes the ratio of signal decay rates in the resonator mode and in the free space modes. It is clear that the measured decay rate $\Gamma_{\rm exp} \neq \Gamma$ when the photon emission rates R_c and R_f decay differently ($\theta \neq 1$). Cases of $\theta = 1$ exist for many atoms excited into only one eigenvector $\vec{\sigma}(0) = \vec{v}_\xi$. Essentially, $\Gamma_{\rm exp} = \Gamma$ holds only when the system decays exactly single exponentially.

Within the range of C_1 and N explored in our experiments, the calculation indicates that $\theta > 1$ ($\theta \lesssim 1$) for the steady state (timed-Dicke state) in the early time dynamics [29]. As a result, $\Gamma_{\rm exp} > \Gamma$ can be seen in Fig. 3(e) for the steady state and $\Gamma_{\rm exp} < \Gamma$ in (f) for the timed-Dicke state. Applying these relations to the observed limit $\Gamma^0_{\rm exp}$ and using $\Gamma \approx \Gamma_f$ as $C_1 \to 0$, our measurements reveal $\Gamma_f < \Gamma^0_{\rm exp} \approx \Gamma_0$, appearing subradiant for the steady state, and $\Gamma_f \gtrsim \Gamma^0_{\rm exp} \gtrsim \Gamma_0$, appearing superradiant for the timed-Dicke state. These decay characteristics of photon emission in free space are consistent with those already discussed in Figs. 2(c) and 2(d).

Moreover, the calculated Γ_f of the steady state, as seen in Fig. 3(e), is significantly below the single atom decay rate Γ_0 and remains nearly constant even when C_1 vanishes. For the timed-Dicke state, $\Gamma_f > \Gamma_0$ for all C_1 as shown in (f).

Experiment and theory comparison—N dependence—We now study the number dependence to further confirm the selective collective emission signatures. Figure 4(a) shows that the measured $\Gamma^0_{\rm exp}/\Gamma_0 \approx 1$ is remarkably

atom-number independent for the steady state, agreeing well with the theoretical calculations. For the timed-Dicke state in Fig. 4(b), Γ^0_{exp} increases with respect to N. This trend is consistent with the calculations although the agreement is worse; see [29] for discussions about the discrepancy.

We attempt to deduce the free space decay rate contribution Γ_f using the experimental data. Here, we rely on the expectation from Eq. (2) that $\Gamma^0_{\mathrm{exp}} \approx \Gamma_f \theta$ when Γ_c is vanishingly small, and apply the value of calculated θ to evaluate $\Gamma_f = \Gamma^0_{\mathrm{exp}}/\theta$. The results are shown in Fig. 4(c). The number dependence indeed gives the signatures of subradiance (suppressed decay rate with increasing N) and superradiance (enhanced decay rate with N) for the steady state and the timed-Dicke state, respectively.

We note that the measured Γ_f are obtained in the limit of vanishing interaction with the microring resonator. For the theoretical calculations under finite C_1, Γ_f becomes slightly more suppressed for the steady state as shown in Fig. 4(c). For the timed-Dicke state and with larger C_1, the decay rate saturates with increasing N.

Finally, we confirm the superradiant scaling for the decay rate in the resonator channel. We calculate $\Gamma_c \approx \Gamma_{\mathrm{exp}} - \Gamma^0_{\mathrm{exp}}$, where we have assumed that $\Gamma_f \theta \approx \Gamma^0_{\mathrm{exp}}$ remains roughly constant within the explored parameter range [29]. The result is shown in Fig. 4(d). The overall trend is consistent with theory, which shows superradiance with a general dependence $\Gamma_c/\Gamma_0 \approx NC_1$ for both the steady state and the timed-Dicke state.

In conclusion, we experimentally and theoretically study selective collective emissions of a dense atomic ensemble coupled to a nanophotonic microring resonator. We demonstrate the dynamics of superradiant decay into a resonator mode, and reveal the subradiant (superradiant) decay signature into other nonguided modes for the steady-state state (the timed-Dicke state). For the latter, a discrepancy is found between theory prediction and measurement result for the timed-Dicke state, which requires further investigations [29]. In the End Matter, we further provide an estimate for the figure of merit of an atom-photon interface exhibiting the selective collective emission behavior. We believe our methodology for characterizing the decay dynamics of a dense atomic ensemble could shed light on future investigations of the collective emission with densely packed quantum emitters, ordered or disordered, coupled to nanophotonic waveguides and resonators.

Acknowledgments—We thank Darrick Chang and Valentin Walther for discussions. We are grateful to Tzu-Han Chang, Dipanjan Das, and Saivirinchi Prabandhakavi for their assistance in the experimental work. X. Z. and C.-L. H. acknowledge support from the AFOSR (Grant No. FA9550-22-1-0031) and the ONR (Grant No. N00014-24-1-2184). D. S. and F. R. are supported by the NSF (Grant No. 2410890-PHY).

Data availability—The data that support the findings of this Letter are openly available [41].

[1] R. H. Dicke, Coherence in spontaneous radiation processes, Phys. Rev. **93**, 99 (1954).
[2] M. Gross and S. Haroche, Superradiance: An essay on the theory of collective spontaneous emission, Phys. Rep. **93**, 301 (1982).
[3] F. Andreoli, M. J. Gullans, A. A. High, A. Browaeys, and D. E. Chang, Maximum refractive index of an atomic medium, Phys. Rev. X **11**, 011026 (2021).
[4] K. Hammerer, A. S. Sørensen, and E. S. Polzik, Quantum interface between light and atomic ensembles, Rev. Mod. Phys. **82**, 1041 (2010).
[5] P. Kómár, T. Topcu, E. M. Kessler, A. Derevianko, V. Vuletić, J. Ye, and M. D. Lukin, Quantum network of atom clocks: A possible implementation with neutral atoms, Phys. Rev. Lett. **117**, 060506 (2016).
[6] E. Pedrozo-Peñafiel, S. Colombo, C. Shu, A. F. Adiyatullin, Z. Li, E. Mendez, B. Braverman, A. Kawasaki, D. Akamatsu, Y. Xiao, and V. Vuletić, Entanglement on an optical atomic-clock transition, Nature (London) **588**, 414 (2020).
[7] M. O. Scully, E. S. Fry, C. H. Raymond Ooi, and K. Wódkiewicz, Directed spontaneous emission from an extended ensemble of N atoms: Timing is everything, Phys. Rev. Lett. **96**, 010501 (2006).
[8] A. A. Svidzinsky, J.-T. Chang, and M. O. Scully, Dynamical evolution of correlated spontaneous emission of a single photon from a uniformly excited cloud of N atoms, Phys. Rev. Lett. **100**, 160504 (2008).
[9] M. O. Scully, Single photon subradiance: Quantum control of spontaneous emission and ultrafast readout, Phys. Rev. Lett. **115**, 243602 (2015).
[10] T. Bienaimé, N. Piovella, and R. Kaiser, Controlled Dicke subradiance from a large cloud of two-level systems, Phys. Rev. Lett. **108**, 123602 (2012).
[11] W. Guerin, M. O. Araújo, and R. Kaiser, Subradiance in a large cloud of cold atoms, Phys. Rev. Lett. **116**, 083601 (2016).
[12] A. Cipris, N. A. Moreira, T. S. do Espirito Santo, P. Weiss, C. J. Villas-Boas, R. Kaiser, W. Guerin, and R. Bachelard, Subradiance with saturated atoms: Population enhancement of the long-lived states, Phys. Rev. Lett. **126**, 103604 (2021).
[13] D. C. Gold, P. Huft, C. Young, A. Safari, T. G. Walker, M. Saffman, and D. D. Yavuz, Spatial coherence of light in collective spontaneous emission, PRX Quantum **3**, 010338 (2022).
[14] G. Ferioli, A. Glicenstein, L. Henriet, I. Ferrier-Barbut, and A. Browaeys, Storage and release of subradiant excitations in a dense atomic cloud, Phys. Rev. X **11**, 021031 (2021).
[15] S. J. Roof, K. J. Kemp, M. D. Havey, and I. M. Sokolov, Observation of single-photon superradiance and the cooperative Lamb shift in an extended sample of cold atoms, Phys. Rev. Lett. **117**, 073003 (2016).

[16] M. O. Araújo, I. Krešić, R. Kaiser, and W. Guerin, Superradiance in a large and dilute cloud of cold atoms in the linear-optics regime, Phys. Rev. Lett. **117**, 073002 (2016).
[17] G. Ferioli, A. Glicenstein, F. Robicheaux, R. T. Sutherland, A. Browaeys, and I. Ferrier-Barbut, Laser-driven superradiant ensembles of two-level atoms near Dicke regime, Phys. Rev. Lett. **127**, 243602 (2021).
[18] L. Ji, Y. He, Q. Cai, Z. Fang, Y. Wang, L. Qiu, L. Zhou, S. Wu, S. Grava, and D. E. Chang, Superradiant detection of microscopic optical dipolar interactions, Phys. Rev. Lett. **131**, 253602 (2023).
[19] A. Goban, C.-L. Hung, J. D. Hood, S.-P. Yu, J. A. Muniz, O. Painter, and H. J. Kimble, Superradiance for atoms trapped along a photonic crystal waveguide, Phys. Rev. Lett. **115**, 063601 (2015).
[20] A. Tiranov, V. Angelopoulou, C. J. van Diepen, B. Schrinski, O. A. D. Sandberg, Y. Wang, L. Midolo, S. Scholz, A. D. Wieck, A. Ludwig, A. S. Sørensen, and P. Lodahl, Collective super- and subradiant dynamics between distant optical quantum emitters, Science **379**, 389 (2023).
[21] P. Solano, P. Barberis-Blostein, F. K. Fatemi, L. A. Orozco, and S. L. Rolston, Super-radiance reveals infinite-range dipole interactions through a nanofiber, Nat. Commun. **8**, 1857 (2017).
[22] R. Pennetta, M. Blaha, A. Johnson, D. Lechner, P. Schneeweiss, J. Volz, and A. Rauschenbeutel, Collective radiative dynamics of an ensemble of cold atoms coupled to an optical waveguide, Phys. Rev. Lett. **128**, 073601 (2022).
[23] C. Liedl, F. Tebbenjohanns, C. Bach, S. Pucher, A. Rauschenbeutel, and P. Schneeweiss, Observation of superradiant bursts in a cascaded quantum system, Phys. Rev. X **14**, 011020 (2024).
[24] X. Zhou, H. Tamura, T.-H. Chang, and C.-L. Hung, Trapped atoms and superradiance on an integrated nanophotonic microring circuit, Phys. Rev. X **14**, 031004 (2024).
[25] A. Asenjo-Garcia, M. Moreno-Cardoner, A. Albrecht, H. J. Kimble, and D. E. Chang, Exponential improvement in photon storage fidelities using subradiance and "selective radiance" in atomic arrays, Phys. Rev. X **7**, 031024 (2017).
[26] S. Grava, Y. He, S. Wu, and D. E. Chang, Renormalization group analysis of near-field induced dephasing of optical spin waves in an atomic medium, New J. Phys. **24**, 013031 (2022).
[27] M. O. Scully, Collective Lamb shift in single photon Dicke superradiance, Phys. Rev. Lett. **102**, 143601 (2009).
[28] M. O. Scully and A. A. Svidzinsky, The super of superradiance, Science **325**, 1510 (2009).
[29] See Supplemental Material at http://link.aps.org/supplemental/10.1103/cdd5-r7h4, which includes Refs. [30–32], for details on the theoretical model, numerical calculations, decay rate measurement, and data analysis.
[30] J. Kumlin, S. Hofferberth, and H. P. Büchler, Emergent universal dynamics for an atomic cloud coupled to an optical waveguide, Phys. Rev. Lett. **121**, 013601 (2018).
[31] R. Pennetta, D. Lechner, M. Blaha, A. Rauschenbeutel, P. Schneeweiss, and J. Volz, Observation of coherent coupling between super- and subradiant states of an ensemble of cold atoms collectively coupled to a single propagating optical mode, Phys. Rev. Lett. **128**, 203601 (2022).
[32] A. F. Oskooi, D. Roundy, M. Ibanescu, P. Bermel, J. Joannopoulos, and S. G. Johnson, Meep: A flexible free-software package for electromagnetic simulations by the FDTD method, Comput. Phys. Commun. **181**, 687 (2010).
[33] X. Zhou, H. Tamura, T.-H. Chang, and C.-L. Hung, Coupling single atoms to a nanophotonic whispering-gallery-mode resonator via optical guiding, Phys. Rev. Lett. **130**, 103601 (2023).
[34] G. Ferioli, A. Glicenstein, I. Ferrier-Barbut, and A. Browaeys, A non-equilibrium superradiant phase transition in free space, Nat. Phys. **19**, 1345 (2023).
[35] D. A. Suresh, X. Zhou, C.-L. Hung, and F. Robicheaux, Collective emission and selective-radiance in atomic clouds and arrays coupled to a microring resonator, arXiv:2503.21121.
[36] R. J. Bettles, S. A. Gardiner, and C. S. Adams, Enhanced optical cross section via collective coupling of atomic dipoles in a 2D array, Phys. Rev. Lett. **116**, 103602 (2016).
[37] R. T. Sutherland and F. Robicheaux, Collective dipole-dipole interactions in an atomic array, Phys. Rev. A **94**, 013847 (2016).
[38] G. Facchinetti, S. D. Jenkins, and J. Ruostekoski, Storing light with subradiant correlations in arrays of atoms, Phys. Rev. Lett. **117**, 243601 (2016).
[39] E. Shahmoon, D. S. Wild, M. D. Lukin, and S. F. Yelin, Cooperative resonances in light scattering from two-dimensional atomic arrays, Phys. Rev. Lett. **118**, 113601 (2017).
[40] The background cannot be fully eliminated by pulsing off the trap light during the probe duration due to fluorescence from the silicon nitride.
[41] X. Zhou, D. A. Suresh, F. Robicheaux, and C.-L. Hung, Data for: Selective Collective Emission from a Dense Atomic Ensemble Coupled to a Nanophotonic Resonator, Purdue University Research Repository, 10.4231/91CW-JX57.

End Matter

Figure of merit—In contrast to single-emitter interfaces, the figure of merit of a collective atom-photon interface is not R_c/R_f because of the selective collective emission dynamics. Instead, we should compare the integrated photon emission into the microring and free space, $P_{c,f} = \int_0^\infty R_{c,f}(t)dt$, and aim to maximize P_c while minimizing P_f. We define the figure of merit as $P_c/P_f \approx R_c(0)/[R_f(0)\theta]$, where we have used the early-time dynamics as an approximation: $P_c \approx \int_0^\infty R_c(0)e^{-\Gamma_{\rm th}t}dt \approx R_c(0)/(\Gamma_c + \Gamma_f\theta)$ and, similarly, $P_f \approx R_f(0)/(\Gamma_c/\theta + \Gamma_f)$ as R_f decays approximately with a rate $\Gamma_{\rm th}/\theta$. For an ensemble of atoms coupled to the microring, we find that the ratio $R_c(0)/R_f(0) \approx \Gamma_c/\Gamma_0 \approx NC_1$ holds for both the steady

state and the timed-Dicke state [35]. This suggests that the figure of merit can be estimated as $P_c/P_f \approx NC_1/\theta$. Here, an additional factor θ^{-1} appears when compared with the conventional expectation $P_c/P_f \approx NC_1$ for emitters superradiantly couple to a photon-emitter interface but independently decay to free space. It thus becomes obvious that the timed-Dicke state (with $\theta \lesssim 1$) will still be a better state for photon storage and retrieval than the steady state (with $\theta > 1$), even though the latter shows apparent subradiant decay dynamics in the free space modes. This somehow counterintuitive conclusion results from the fact that the steady state is mainly populated by eigenmodes that appear darker to the microring due to optical pumping.

Last, we comment that the figure of merit will be greatly improved with an ordered atom array coupled to a microring resonator, as $R_c(0)/R_f(0) \gg NC_1$ increases either polynomially with the atom number N in an array with open ends or exponentially with a closed circular array [25] trapped on a microring [35].